

STUDY OF  $K\alpha$  X RAYS FROM Al, Sc, AND Ti  
FOLLOWING BROMINE-ION BOMBARDMENT

by

KEITH A. JAMISON

B.S., Kansas State University, 1973

---

A MASTER'S THESIS

submitted in partial fulfillment of the

requirements for the degree

MASTER OF SCIENCE

Department of Physics

KANSAS STATE UNIVERSITY  
Manhattan, Kansas

1975

Approved by:

  
Major Professor

LD  
2668  
T4  
1975  
J34  
C-2  
Document

## TABLE OF CONTENTS

LIST OF TABLES . . . . .	11
LIST OF FIGURES . . . . .	111
ACKNOWLEDGMENT . . . . .	iv
I. INTRODUCTION . . . . .	1
II. EXPERIMENTAL TECHNIQUE . . . . .	7
A. BROMINE BEAM . . . . .	7
B. JOHANSSON CRYSTAL . . . . .	11
C. X-RAY MEASUREMENT . . . . .	14
D. CALIBRATION . . . . .	17
E. DATA ANALYSIS . . . . .	18
III. DISCUSSION . . . . .	26
A. ALUMINUM . . . . .	26
B. SCANDIUM . . . . .	27
C. TITANIUM . . . . .	30
IV. CONCLUSION . . . . .	36
REFERENCES . . . . .	38
APPENDIX . . . . .	44
ABSTRACT	

# LIST OF TABLES

I.	Experimental Energies and Wavelengths for $K\alpha$	
	Satellites Produced by Br Bombardment . . . . .	40
II.	Effects of M-shell Vacancies on Al $K\alpha$	
	Satellite Peak Energies . . . . .	41
III.	Effects of M-shell Vacancies on Sc $K\alpha$	
	Satellite Peak Energies . . . . .	42
IV.	Effects of M-shell Vacancies on Ti $K\alpha$	
	Satellite Peak Energies . . . . .	43

# LIST OF FIGURES

Fig. 1	Br + Ti Spectrum by Kast <u>et al.</u> . . . . .	5
Fig. 2	Schematic of Van de Graaff . . . . .	10
Fig. 3	Reflective Focusing by the Johansson Method . . . . .	13
Fig. 4	Target Chamber . . . . .	16
Fig. 5	X-ray Spectrum of Br + Al . . . . .	20
Fig. 6	X-ray Spectrum of Br + Sc . . . . .	22
Fig. 7	X-ray Spectrum of Br + Ti . . . . .	24
Fig. 8	M-shell Shift for Scandium . . . . .	29
Fig. 9	M-shell Shift for Titanium . . . . .	32

## ACKNOWLEDGMENTS

I would like to thank my wife, Carla, for her love and support.

I wish to thank my major professor, Pat Richard, for his efforts in the lab, his guidance, and his encouragement throughout the time that I have been in graduate school, and especially for his help with this thesis.

I am indebted to my co-workers, Dr. Robert Kauffman and Mr. Clifford Woods for their aid in this experiment.

I would like to thank Dea Richard for her efforts in typing and attention to countless details in this thesis and in the published form of this experiment.

I would also like to acknowledge the financial support of the U. S. Energy Research and Development Administration under Contract No. AT(11-1)-2130.

## I. INTRODUCTION

In recent years several differences have been noted between the x-ray spectra produced by proton bombardment as compared with heavy-ion bombardment. As early as 1934 Coates<sup>1)</sup> reported measurements of x-ray production cross sections for several targets bombarded with 2.4 MeV mercury ions. Coates made an important observation that the x rays were not characteristic of either beam or target. Interest in x-ray spectra from inner-shell ionization by high energy, heavy ion beams developed again when a shift to higher energy of the  $K\alpha$  and  $K\beta$  x-ray lines<sup>2,3)</sup> was observed with an oxygen beam as the projectile. The detector in these experiments was a liquid-nitrogen-cooled Si(Li) detector, with a resolution of about 200 eV at 6 keV. The improved resolution of a Bragg reflecting crystal spectrometer showed structure within the heavy-ion induced spectra of target  $K\alpha$  x rays.<sup>4,5)</sup> These first spectra were taken for the targets of Al and Fe with a typical resolution of a few electron volts. The structure or satellites in these  $K\alpha$  spectra has been interpreted as an L-shell vacancy effect. The presence of an L-shell vacancy in an atom changes the energy levels so that atoms with one K-shell vacancy and different numbers of L-shell vacancies will emit  $K\alpha$  x rays with different energies. In many cases<sup>6,7)</sup> these x rays can be resolved into several distinct peaks. The notation used in the thesis is to denote the peaks by  $K\alpha L^n$  where  $n$  is the number of L-shell vacancies present at the time of x-ray decay. The relative intensities of the  $K\alpha L^n$  peaks are found to be a measure of the population distribution of

L-shell vacancies present at the time of x-ray emission.<sup>8)</sup> The relative ionization probabilities  $I_n$  are related to the relative intensities  $R_n$  of the  $K\alpha L^n$  x-ray peaks through the relation  $I_n = R_n / \omega_n$  where  $\omega_n$  is the effective fluorescence yield for the configuration. Considerable attention has been given to the distribution of the relative intensities<sup>9-11)</sup> for many combinations of projectile and target. These papers suggest that for a collision which produces a K-shell vacancy there is a non-negligible probability  $P_L$  that one L-shell vacancy will also be produced. A collision causing a vacancy in the K-shell of the target will in essence be a zero impact parameter collision for the L-shell; therefore  $P_L$  is interpreted as the ionization probability at zero impact parameter. If one assumes  $P_L$  to be a constant for all electrons with the same binding energy and that the production of L-shell vacancies are independent events, then one would expect a binomial distribution in the relative intensities of the  $K\alpha L^n$  ionization states. The single K-shell multiple L-shell ionization ratios can be described by making the above assumptions and by fitting the relative intensity distribution for ionization to a binomial distribution with  $P_L$  as the fitting parameter. It also has been shown that the  $K\alpha L^n$  peaks are a combination of many closely spaced lines.<sup>8,12)</sup> This has been interpreted as evidence for multiplet splitting. Other experiments<sup>13,14)</sup> have exhibited a shift to higher energy of L x rays due to the degree of M-shell vacancies present. All these effects of target x rays must be considered in the light that they are single collision events since the nominal beam currents and focusing will almost never produce more than one collision with the same target atom in the time

required for that atom to decay.

In a recent Physical Review Letter, Kast et al.<sup>15)</sup> extended the study of K $\alpha$  satellites to bromine beams with targets of Mn and Ti. They did not resolve any K $\alpha$  satellite structure in Bragg crystal spectra. Fig. 1 shows a typical spectrum obtained by Kast et al. of Ti K $\alpha$  x rays following impact with 96 MeV Br. They suggest that a greater variation in M-shell vacancies broadens the single K-, multiple L-shell peaks to the point where no structure can be seen with their reported resolution. The initial purpose of this experiment was to see if structure could be resolved by using higher resolution.

In this thesis measurements of resolved structure in K $\alpha$  x-ray satellites from Al, Sc, and Ti following Br-ion bombardment are reported. The observed energies and relative intensities have been extracted and tabulated. By averaging the relative intensities of the satellite peaks an average number of L-shell vacancies present at the time of x-ray emission can be determined. Under 31 MeV bromine-ion bombardment this average number of L-shell vacancies is seen to decrease with increasing target atomic number. Peak energies for different numbers of L-shell vacancies produced in the Br bombardments are compared to Hartree-Fock<sup>16,17)</sup> single configuration self consistent field calculations using screened hydrogenic wave functions and to measured energies obtained by oxygen<sup>18,19)</sup> impact. These results indicate that the number of M-shell vacancies present at the time of x-ray emission increases with increasing L-shell vacancies for the Sc and Ti targets. This effect is not seen in Al, possibly because there are so few M-shell electrons. The energy differences between single K-, multiple L-shell

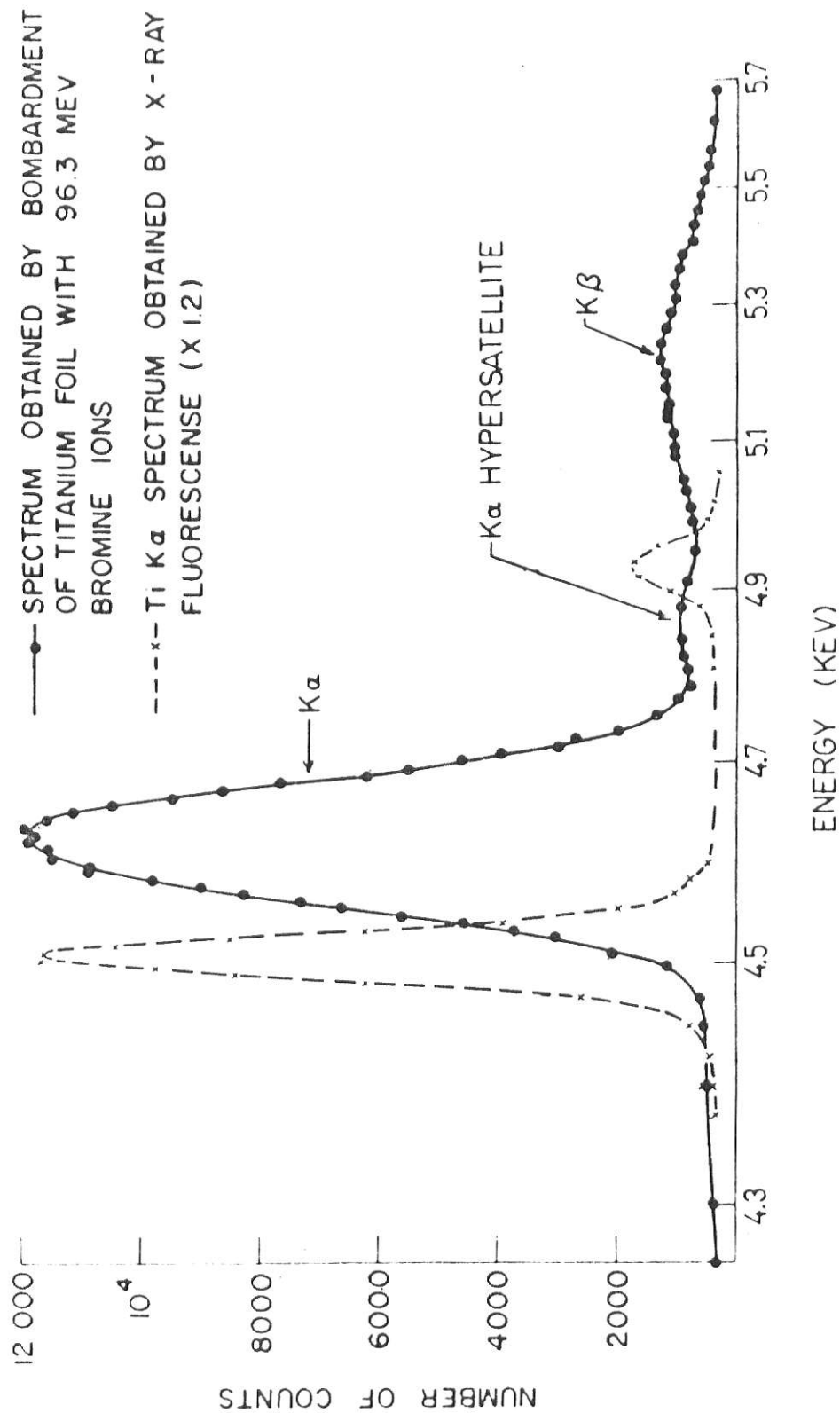
Figure 1: A typical x-ray spectrum of Ti  $K\alpha$  and  $K\beta$  satellite lines taken by Kast et al.<sup>15)</sup> The x rays following Br ion bombardment were wavelength analyzed by a graphite mosaic crystal spectrometer with a reported resolution of 44 eV. (Reprinted from Kast et al., Phys. Rev. Lett. 32, 697 (1974)).

**THIS BOOK  
CONTAINS  
NUMEROUS PAGES  
WITH ILLEGIBLE  
PAGE NUMBERS  
THAT ARE CUT OFF,  
MISSING OR OF POOR  
QUALITY TEXT.**

**THIS IS AS RECEIVED  
FROM THE  
CUSTOMER.**

**THIS BOOK  
CONTAINS  
NUMEROUS PAGES  
WITH DIAGRAMS  
THAT ARE CROOKED  
COMPARED TO THE  
REST OF THE  
INFORMATION ON  
THE PAGE.**

**THIS IS AS  
RECEIVED FROM  
CUSTOMER.**



peaks when produced by O bombardment suggest that this is a collisional effect. A collisional effect cannot be explained by the decay mechanisms of a separated atom. This excludes many important effects which follow a collision as being the cause of this effect. Fluorescence yield, Auger rates, and Coster-Kronig subshell rearrangement will not offer an acceptable explanation for the different trends in target M-shell vacancies following Br and O impact. Two areas which might yield an explanation are target recoil effects and molecular promotion.

## II. EXPERIMENTAL TECHNIQUE

### A. Bromine Beam

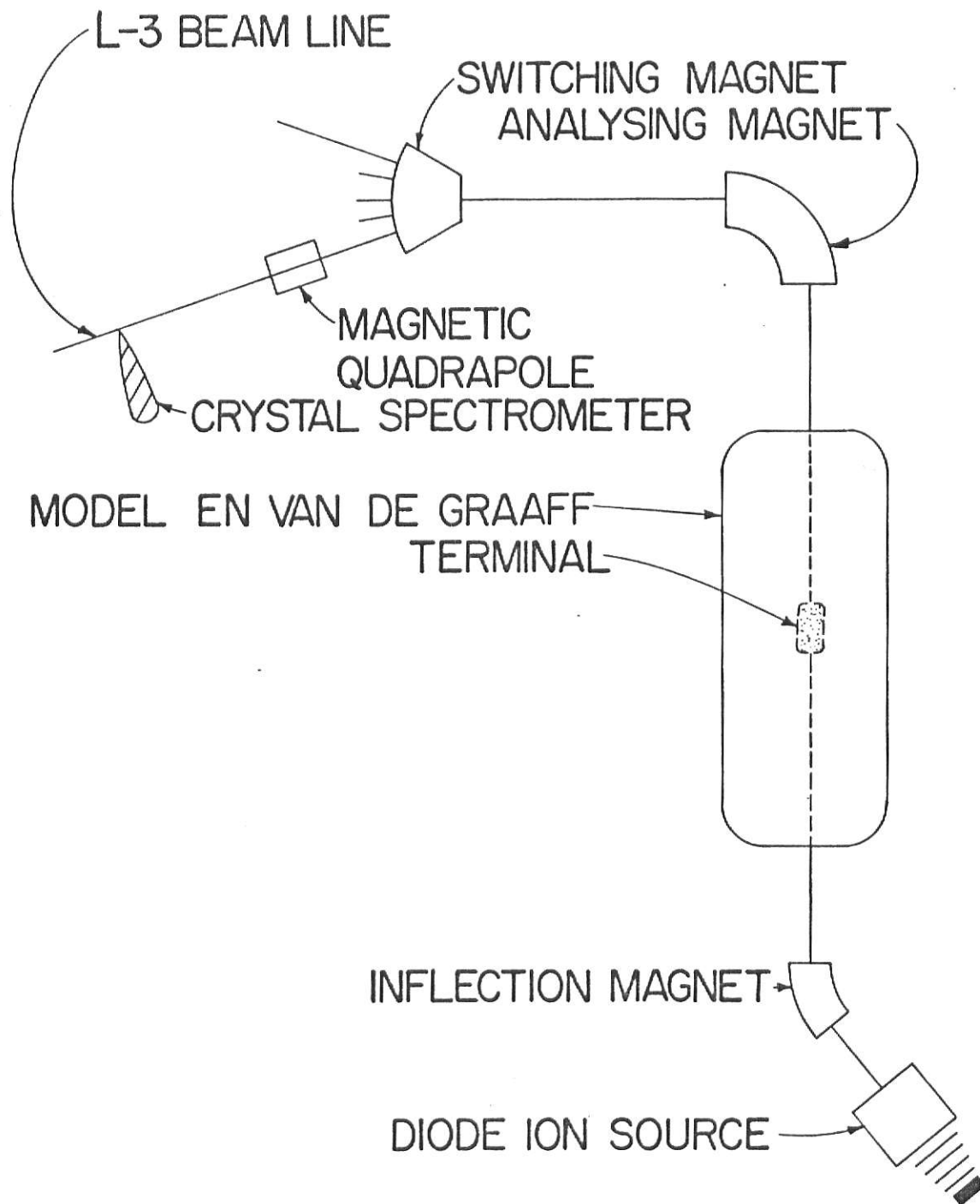
A beam of bromine ions accelerated by the Kansas State University tandem Van de Graaff to an energy of 31 MeV was bombarded on thick targets of Al, Sc, and Ti. The resulting target x rays were wavelength analyzed by a Bragg reflecting crystal spectrometer. The description of the experiment is separated into four sections. The first section is a time-of-flight description of the bromine-ion beam. The second discusses the focusing properties of a Johansson curved crystal. The third explains the x-ray measurements with the four-inch curved crystal spectrometer, and the fourth section gives the details of calibrating the x-ray spectra that were taken.

Bromine is a volatile, corrosive element which must be handled with care. Since the bromine vapor pressure at room temperature is less than one atmosphere the transfer of liquid must be done in a well-vented hood. Bromine is only two percent soluble in water and much heavier than water, so a mixture of bromine and water is much safer to handle than pure bromine. Approximately 50 cc of bromine and 200 cc of water are put into a flask connected to a vacuum roughing pump and to the diode-ion source via a needle valve. By opening the flask to the roughing pump for a short time the pressure is reduced enough for the bromine to boil beneath the layer of water. The process fills the remaining volume of the flask with a high concentration of bromine vapor. The roughing pump is then closed and the needle valve is opened, thus admitting this vapor to the hydrogen arc. In

this plasma, negative bromine-ions are formed. They undergo an acceleration of 55 KV from the source extractor and are mass analyzed by the inflection magnet.

Two approximately equal intensity beams are seen at this point due to the 49-51 natural abundance ratio of  $\text{Br}^{81}$  and  $\text{Br}^{79}$ . One of these beams was then accelerated toward the terminal of the 6 MV EN-27 tandem Van de Graaff which was charged at a positive 4.41 million volts. In the terminal the negative bromine-ion is stripped of several outer electrons by passing through a region containing a low pressure of oxygen gas. The now positive bromine-ion drifts through the terminal and is accelerated again. The beam is energy analyzed by means of a  $90^\circ$  analyzing magnet. This magnet is used for energy calibration of the beams, for slit feedback control of the terminal voltage, and also separates the charge states of the Br beam. The highest intensity beam analyzed was that of the  $6^+$  31 MeV ions, although sizable beams (.1 - 1.0  $\mu\text{A}$ ) of  $4^+$  22 MeV,  $5^+$  26 MeV, and  $7^+$  35 MeV beams could also be obtained by varying the current of the analyzing magnet. The  $6^+$  31 MeV bromine-ions were deflected  $45^\circ$  by the switching magnet into the L-3 beam line. They were then focused by a magnetic quadrupole and collimated by a 4mm circular aperture. Figure 2 shows a schematic of the EN Van de Graaff with the components discussed above. The last step for the bromine-ion is the collision with the thick metallic target. This is of dual importance. First, the ion-atom collision will, with some finite probability, produce a target  $K\alpha$  x ray. Second, the charge collected on the insulated target is metered by a Brookhaven Instruments Corporation current integrator to normalize data points to the

Figure 2: A schematic of the Kansas State University 6 MV tandem Van de Graaff showing the features discussed in the text.



same number of bromine ions striking the target.

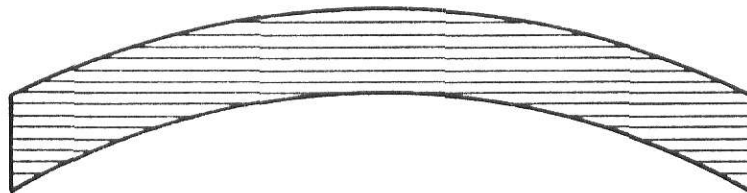
### B. Johansson Crystal

To obtain sufficiently high resolution to resolve the  $K\alpha L^n$  x rays studied in this paper it is necessary to wavelength-analyze the radiation produced with a reflecting crystal. In doing so the reflected x rays will constructively interfere at integral multiples,  $n\lambda = 2d \sin\theta$ , by the Bragg law of reflection.  $\lambda$  is the wavelength of the x ray and  $\theta$  is the angle between the incident path of the x ray and the crystal planes. All the spectra obtained for this thesis were in first order; i.e.,  $n=1$ .

In order to have a large enough solid angle to measure small intensities, a Johansson focusing crystal<sup>20)</sup> is used. Figure 3 shows the focusing properties of this type crystal. The process for making this type of crystal is rather involved. First, the crystal must be annealed and aligned along the proper axis. It is machined (polished) to a circular cylinder form of radius  $2R$ . The final step is to bend the machined crystal to a radius of  $R$ . Referring to the diagram on Fig. 3, the crystal planes are now concentric with radius  $2R$  about center  $O$ . A source is placed on the focal circle at point  $S$ . The detector is then placed at point  $D$  so that arc  $SO$  equals arc  $OD$ . It is a brief geometrical proof to show this gives exact focusing. Choose point  $A$  such that line  $AO$  is a diameter of the focal circle. Now choose any  $B$ , any point on the crystal. Angle  $SBD = \psi$  and angle  $SAD = \psi$  since any two chords from a point subtending the same arc form equal angles. The angle of incidence must equal the angle of reflection and

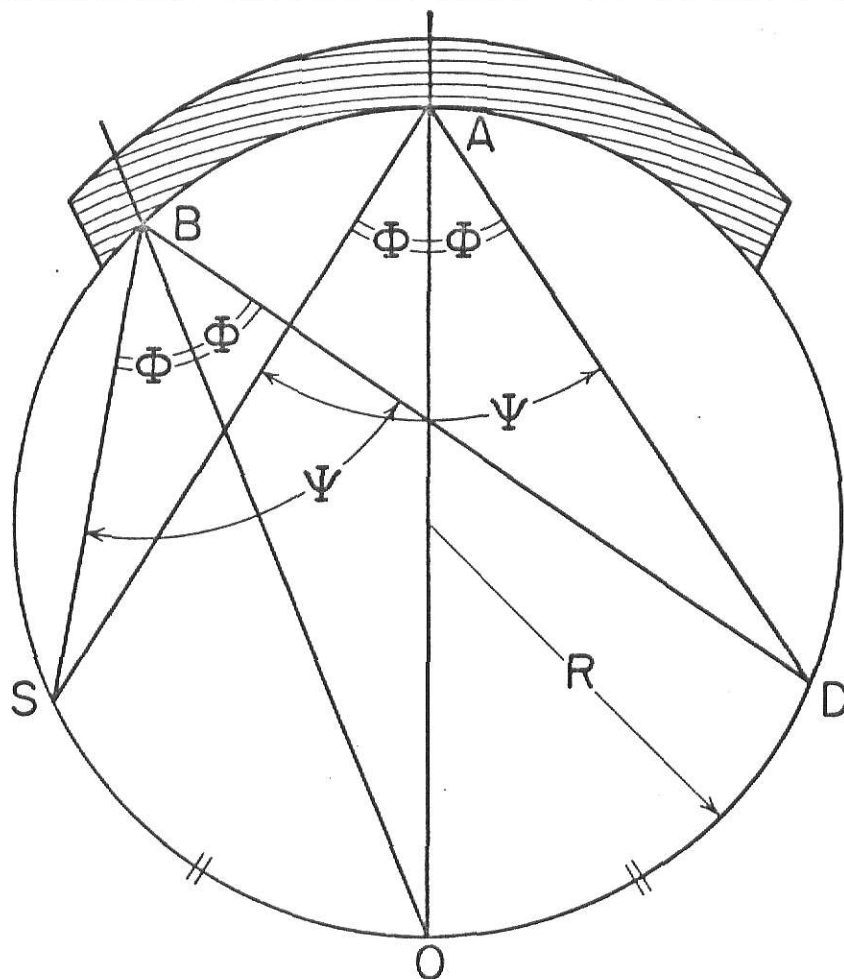
Figure 3: Geometrical view of the focusing properties of the Johansson curved crystal.

# REFLECTIVE FOCUSING BY THE JOHANSSON METHOD



CRYSTAL IS FIRST MACHINED  
TO A RADIUS OF  $2R$

MACHINED CRYSTAL BENT TO RADIUS  $R$

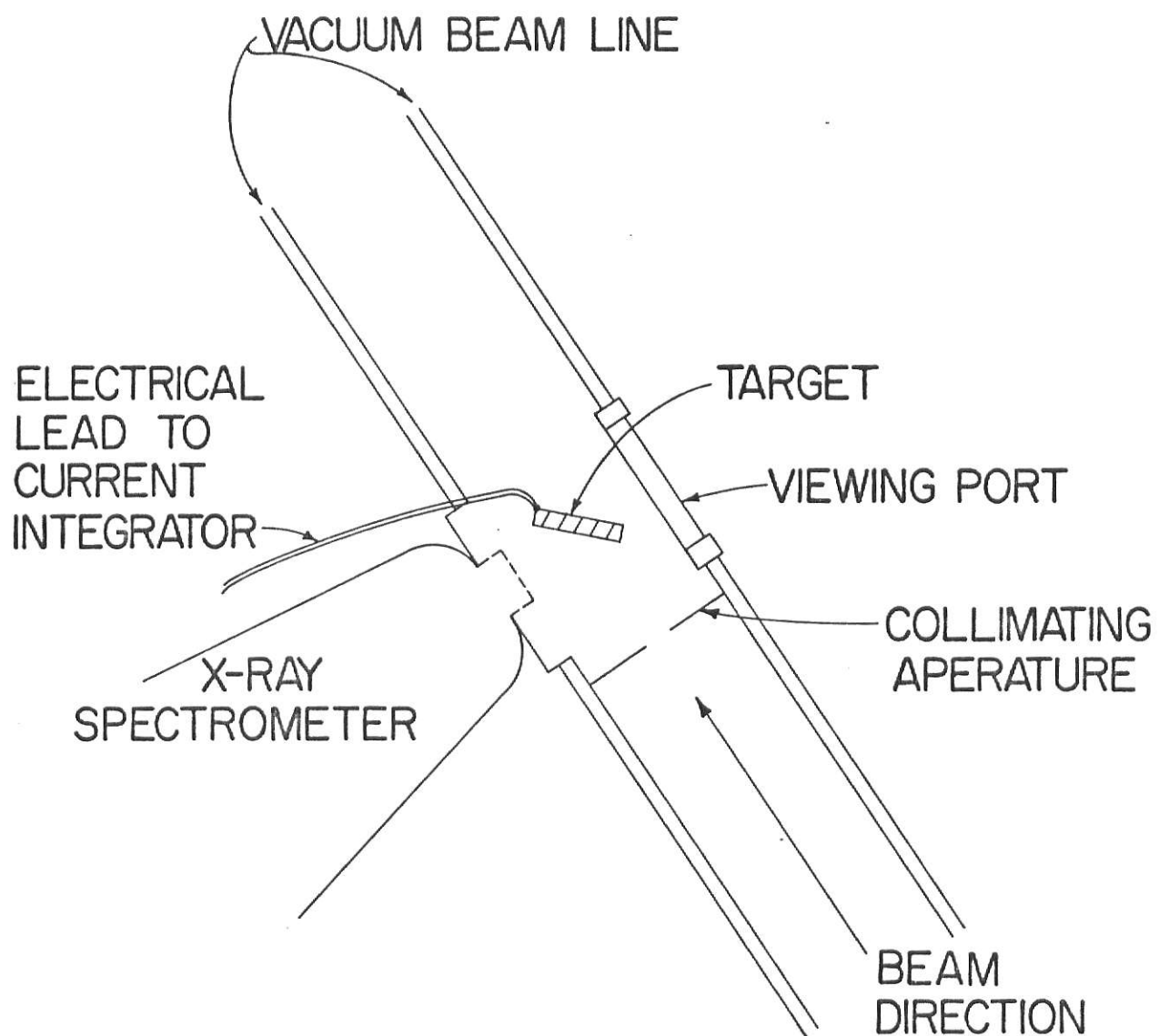


arcs SO and OD are half arc SD; therefore, all four  $\phi$ 's on the diagram are the same. The last thing to prove the Johansson crystal focuses from a point source to a point detector is to show lines OB and OA perpendicular to the reflecting planes. The planes of the crystal are concentric about point O so that they must be perpendicular to any line drawn from point O radially outward. In addition to its exact focusing properties, one should also note that the angle formed by the source and the endpoints of the crystal is constant for any position of S so that the angle of detection in the focal circle plane is constant over the scanning region for theta.

### C. X-Ray Measurement

The four-inch curved crystal spectrometer is placed at  $90^\circ$  with respect to the beam axis as shown in Fig. 4. The targets of Al, Sc, and Ti are lowered into position in front of the spectrometer at a  $45^\circ$  angle to the beam axis. X rays from the target enter the spectrometer and are then Bragg diffracted by the Johansson curved crystal to a flow proportional counter. This x-ray detector uses a P10 gas mixture (10% methane; 90% argon) with a thin  $\sim 5000\text{\AA}$  polypropylene window. The mechanics of the spectrometer are such that in stepping through the desired angles both the source (target) and the proportional counter are kept on the focal circle of the crystal. This requires geared motion of both the crystal and the proportional detector as well as precise angle sweeping of the curved crystal itself. The  $K\alpha$  x rays from Ti and Sc were analyzed in first order ( $\lambda = 2d \sin\theta$ ) using a LiF crystal which has a  $2d$  spacing of  $4.027 \text{ \AA}$ . For Ti the angle  $\theta$

Figure 4: A diagram of the target chamber used for this experiment.



was scanned from  $44^\circ$  to  $40^\circ$ . To study Sc  $K\alpha$  x rays the crystal angle  $\theta$  was scanned over the range  $50^\circ$  to  $45^\circ$ . To analyze the x rays of Al, an ADP crystal with a 2d spacing of  $10.640 \text{ \AA}$  was scanned from  $52^\circ$  to  $46^\circ$ . In all three cases the spectrometer stepping motor was controlled by an on-line PDP-15 computer. At each angular setting of the crystal and detector, the number of x rays was recorded for a given number of microCoulombs of beam integrated from the metal target. The step size for the Ti and Sc spectra was  $.000212 \text{ \AA}$  and for the Al spectra, it was  $.000560 \text{ \AA}$ . In each case approximately 1000 data points were taken. Then each 5 adjacent channels were added together to compress the spectra into 200 channels for later off-line analysis. Each spectrum was repeated at least once and all reproduced to within statistical errors. The number of counts in the  $K\alpha$  satellite peaks is approximately 1000 so each data point can be expected to have an uncertainty of 3%.

#### D. Calibration

Since direct and accurate measurements of the angle of crystal are not easily made, it was necessary to calibrate with x rays of known energy. To accomplish this, the normal  $K\alpha$  and  $K\beta$  lines of Al, Sc, and Ti were induced by  $2.0 \text{ MeV H}^+$  bombardment. The energies of these lines are well known and published by the National Bureau of Standards.<sup>21)</sup> These spectra were taken in exactly the same way as the bromine induced spectra. Much better statistics were obtained here as the uncertainty is 1% for the data points in the normal  $K\alpha$  peak. The full width at half maximum (FWHM) of the  $K\alpha$  peak gives a good indication of the resolution of the spectrometer since natural widths of these lines are much narrower

than the resolution of the spectrometer, approximately .3, .4, and .4 eV for Al, Sc, and Ti, respectively.<sup>22)</sup> For 2.0 MeV  $H^+$  bombardment, the FWHM of the normal  $K\alpha$  lines was 2.5, 11.0, and 24.0 eV for the Al, Sc, and Ti, respectively. Kast et al. reported a resolution of 44 eV for Ti in second order and 32 eV for Mn in third order using a graphite mosaic crystal spectrometer.

#### E. Data Analysis

Figures 5, 6, and 7 show the spectra of Al, Sc, and Ti, respectively for Br and  $H^+$  excitation. In each case a proton calibration spectrum is overlaid with the Br induced spectrum. Each dot of the Br spectrum represents the sum of five data points taken by stepping the crystal and detector angles. The notation used to identify each peak is  $K\alpha L^n$ . This notation describes the vacancies present just prior to the  $K\alpha$  x-ray emission.  $K\alpha L^3$ , for example, refers to x-ray emission from an initial state with one vacancy in the K-shell and two vacancies in the L-shell. Following the emission of an x ray there are three vacancies in the L-shell and a full K-shell. To accurately extract the peak energies and relative intensities an  $X^2$  fit to the data was performed off line on background of the PDP-15 computer. The fitting function was the sum of six Gaussian peaks plus a constant background. Each of the Gaussian peaks had three variable parameters, position, height, and width at  $1/e$  times height. In all 19 parameters were allowed to vary and quite good fits to the data were obtained. The final parameters of the fitting program together with the energy calibration from the proton induced spectra were used to obtain the energies,

Figure 5: Aluminum  $K\alpha$  x-ray spectra resulting from collisions with 31-MeV Br ions and 2 MeV  $H^+$ . The resolution of the Johansson curved crystal spectrometer is 2.5 eV. The  $H^+$  induced spectrum contains approximately 20 times as many counts as the Br induced spectra. The Al K absorption edge is due to the self absorption in the thick target.

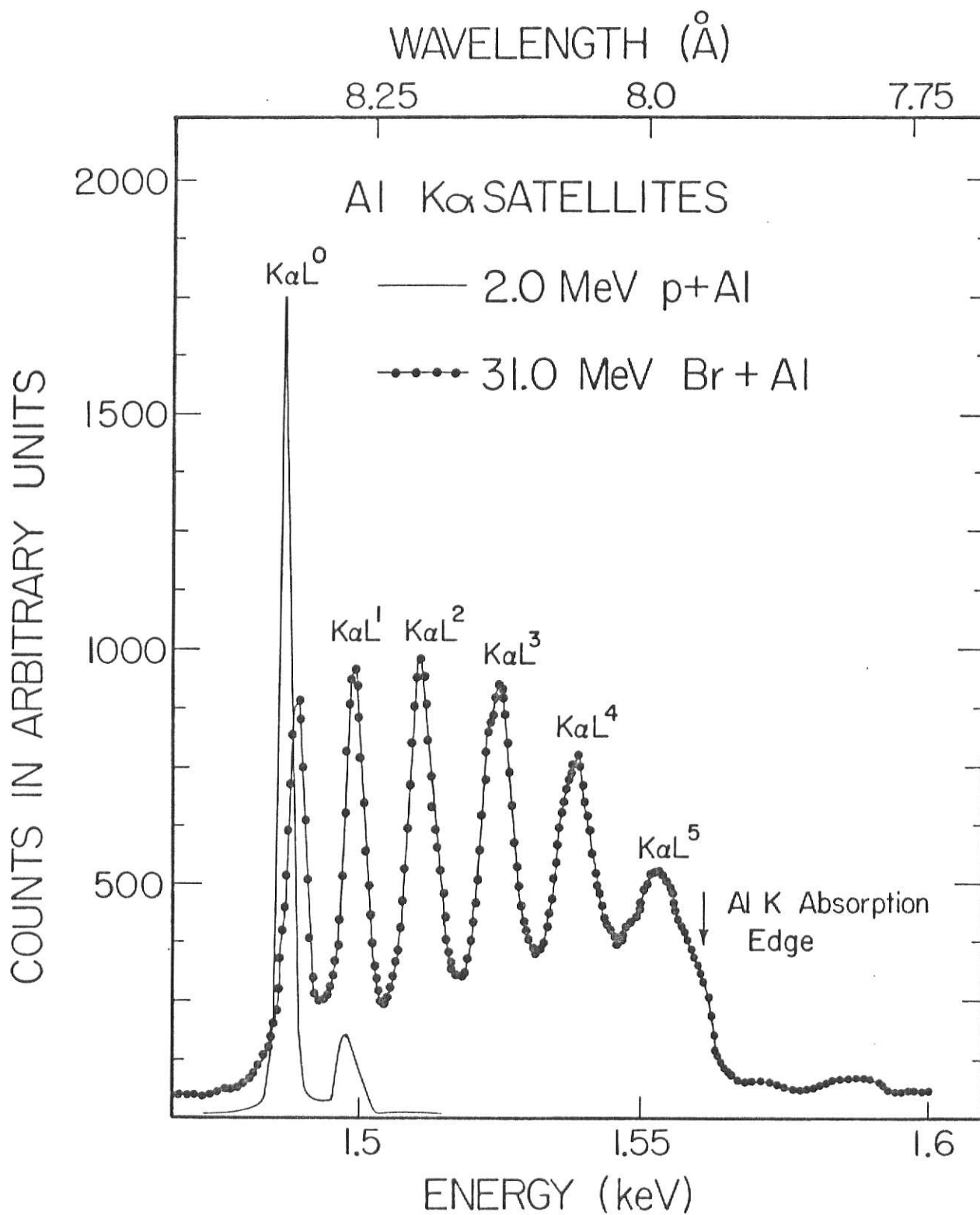


Figure 6: Scandium  $K\alpha$  x-ray spectra after collisions with 31-MeV Br ions and 2 MeV  $H^+$ . The resolution of these spectra is 11 eV. The  $H^+$  induced spectrum contains approximately 15 times as many counts as the Br induced spectrum.

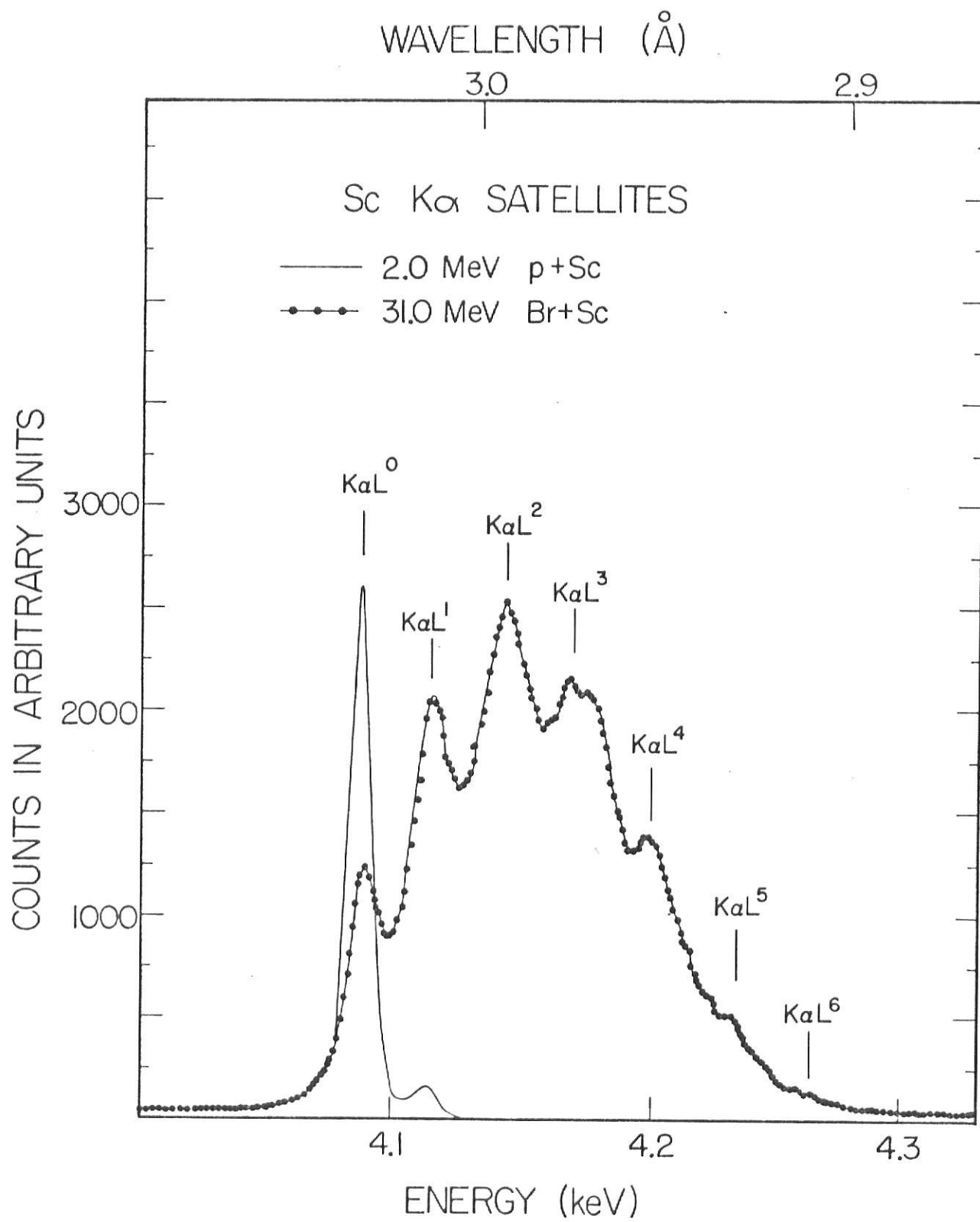
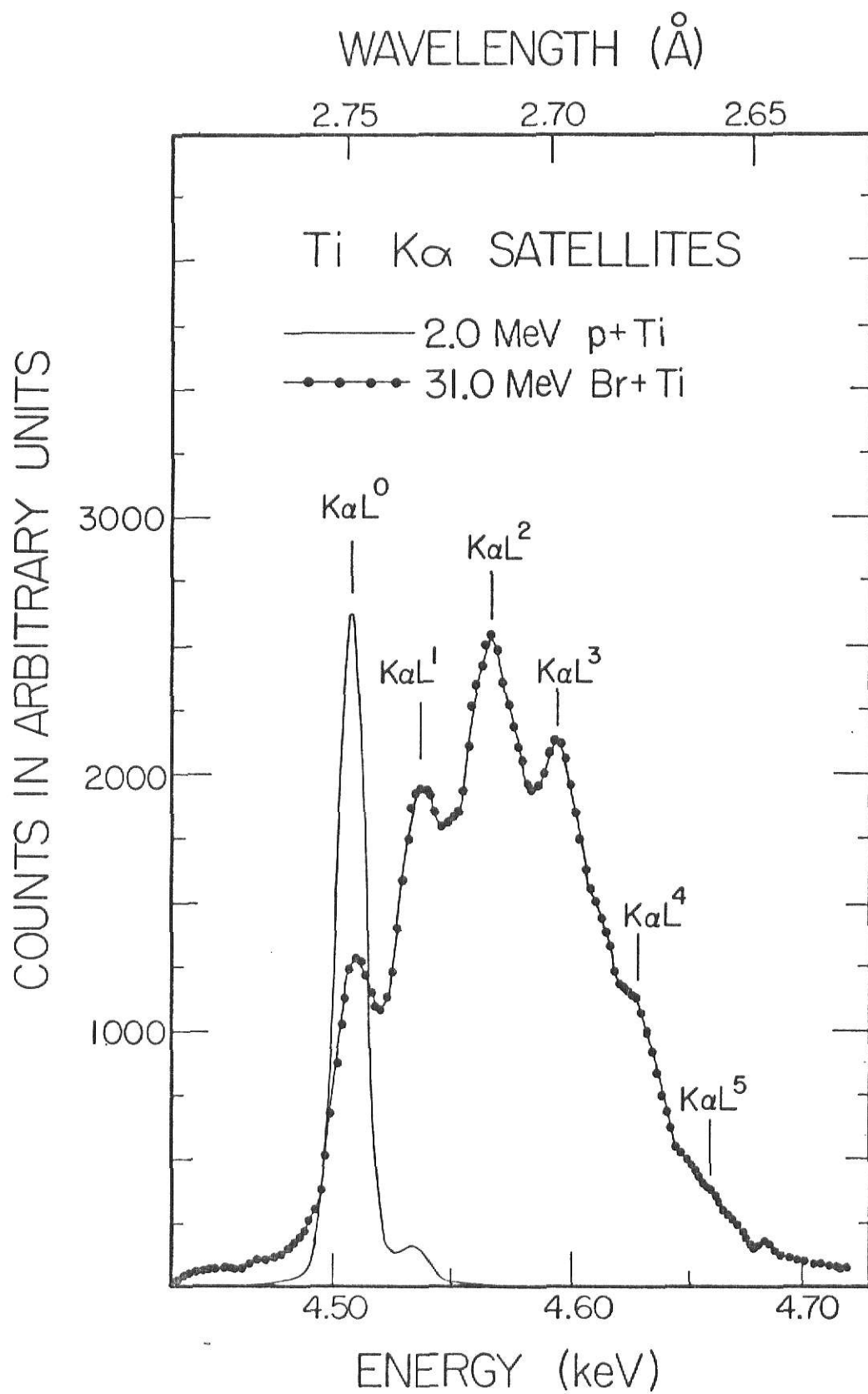


Figure 7: Titanium  $K\alpha$  x-ray spectra after collisions with 31-MeV Br ions and 2 MeV  $H^+$ . The resolution of these spectra is 24 eV. The  $H^+$  induced spectrum contains approximately 15 times as many counts as the Br induced spectrum.



wavelengths, relative intensities and average L-shell vacancies listed in Table I.

The second part of the analysis consisted of extensive Hartree-Fock calculations performed with the Froese-Fischer<sup>16)</sup> Hartree-Fock (HF) computer program. The HF program performed single-configuration, self-consistent field calculations and all wave functions were assumed to be screened hydrogenic. The calculations were approximately .5% too low so that each of the HF energies for a given target and configuration was normalized by the amount needed to correct the normal line calculation to its accepted energy. Defect configurations were then calculated for states having 1 to 5 vacancies in the L-shell present just before the time of x-ray emission. All transitions were assumed to be 1s-2p with a full 2s level since Coster-Kronig sub-shell rearrangements are expected to fill that level much faster than the atom can decay by x-ray emission. At this point we will define an energy shift as being the difference in energy of the observed line and the normalized HF energy calculated with all M-shell electrons present. This quantity is tabulated in Tables II, III, and IV. The shift is calculated for satellite peak energies of both Br and O induced spectra. The final set of energy calculations was performed for states with a different number of M-shell electrons for each of the L-shell defect configurations for each of the targets. Although time and computer money prevented the calculation of all combinations of L-shell and M-shell vacancies, a sufficient number was done to determine a trend and to extrapolate the M-shell defect energies needed for the analysis.

### III. DISCUSSION

#### A. Aluminum

As tabulated in Table I, the average number of L-shell vacancies present at the time of x-ray emission from Al following bromine-ion bombardment is 2.7 with all peaks showing nearly equal intensity and  $K\alpha L^2$ ,  $K\alpha L^3$ , and  $K\alpha L^4$  having relative intensities equal to within statistical uncertainty. The relative intensity of the  $K\alpha L^5$  peaks may be somewhat affected by the self-absorption edge at 1.56 keV. Also, the normal  $K\beta$  line lies within the peak designated as  $K\alpha L^5$ . Normal  $K\beta$  intensity is expected to be small so no attempt is made to correct for these two effects. The resolution (FWHM of the  $K\alpha L^0$  peak) is about 4 eV or about 1.6 times the resolution of the spectrometer so that the bromine induced lines are broadened to some extent with respect to the  $H^+$  induced lines.

Table II shows the effect of M-shell vacancies on the  $K\alpha L^n$  peak positions. Column 2 of the table shows the shift from the normal Hartree-Fock calculations to the actual energy observed. Column 3 shows the number of M-shell vacancies required to explain this energy shift. The configurations used to calculate these energies were  $(1s)^2 (2s)^2 (2p)^{6-n} (3s)^{2-m}$  to  $(1s)^1 (2s)^2 (2p)^{5-n} (3s)^{2-m}$  where n designates the number of L-shell vacancies and m refers to the number of M-shell vacancies. The Al data show no real trend in M-shell vacancies. The number of M-shell vacancies required to explain the observed energy of the  $K\alpha L^n$  peaks is nearly constant for all of the L-shell ionization peaks. In fact, this is what one might expect considering that a K-

shell collision must be a nearly head-on collision for the M-shell.

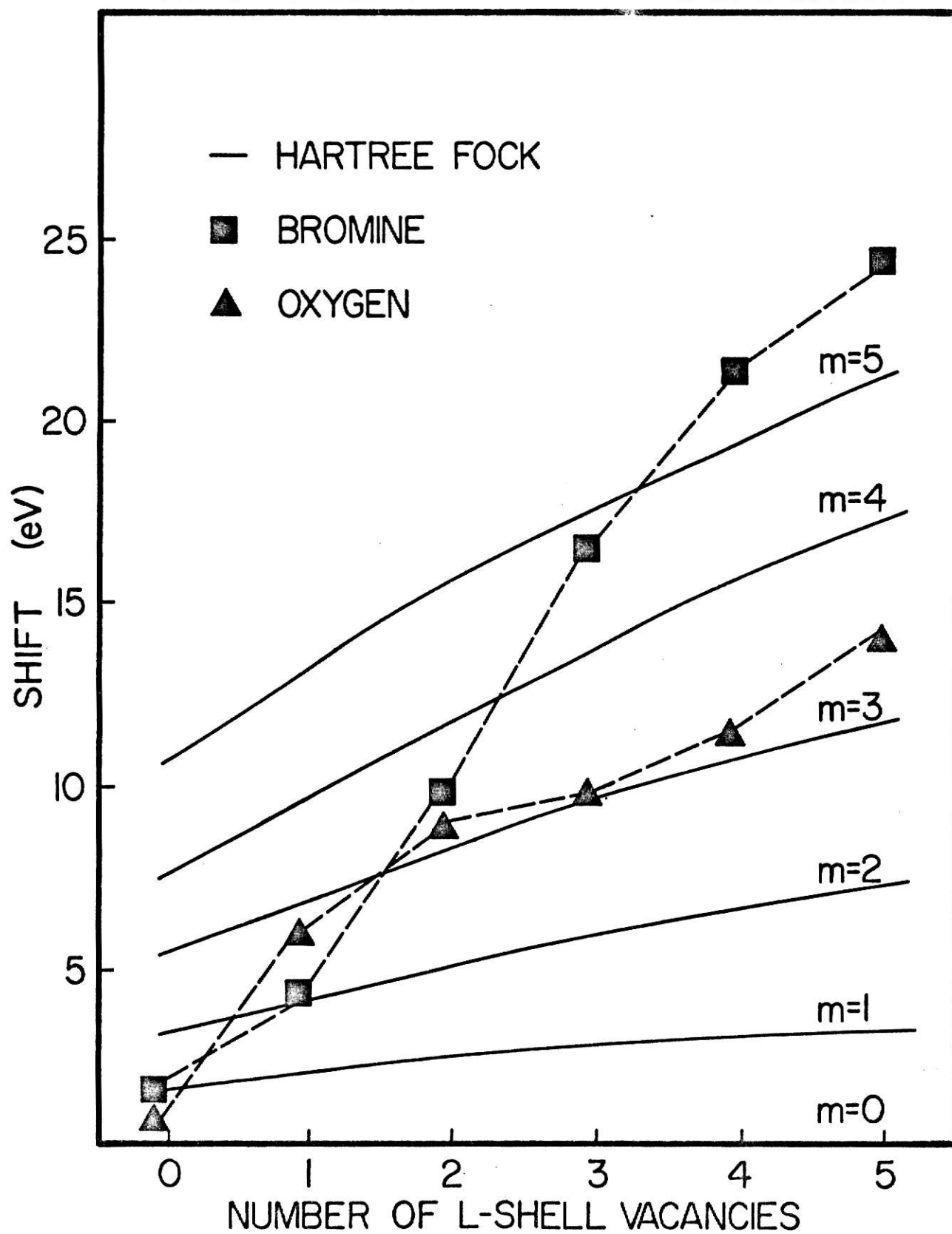
## B. Scandium

Again referring to Table I, Sc has an average of 2.4 L-shell vacancies present at the time of x-ray emission. The largest of the  $K\alpha L^n$  peaks is  $K\alpha L^2$  which has nearly 30% of the  $K\alpha$  x-ray yield. The relative intensities more closely resemble the binomial distributions expected if one assumes  $P_L$  (probability of removing an L-shell electron during collision which produces a K-shell vacancy) is constant and that the production of L-shell vacancies is an independent event. This differs greatly from the nearly equal relative intensities of Al satellite peaks. The resolution (FWHM) of these peaks is 20 eV so that the  $K\alpha L^n$  peaks are very nearly double the resolution of the spectrometer. Even with this increased line width the first five satellite peaks are clearly discernible, and the sixth can be evaluated with the  $X^2$  fit to overlapping Gaussian peaks.

Table III shows the effect of M-shell vacancies for Sc. Tabulated together with the Br shift is the shift of oxygen induced  $K\alpha$  satellite lines. This oxygen shift is the difference in the experimentally measured energies by Hodge et al.<sup>10)</sup> and normalized HF calculations with a full M-shell. Also tabulated is the number of M-shell vacancies required to explain this energy shift for bromine and for oxygen. Figure 8 shows this effect graphically. Plotted vertically is x-ray energy minus the normalized HF calculation for a given satellite peak having all M-shell electrons present. Along the horizontal x axis is the number of L-shell vacancies present just prior to

Figure 8: The shift of the scandium  $K\alpha L^n$  peak energies for Br and O bombardment compared to H-F calculations for  $m$  vacancies in the scandium M-shell.

# M-SHELL SHIFT FOR SCANDIUM



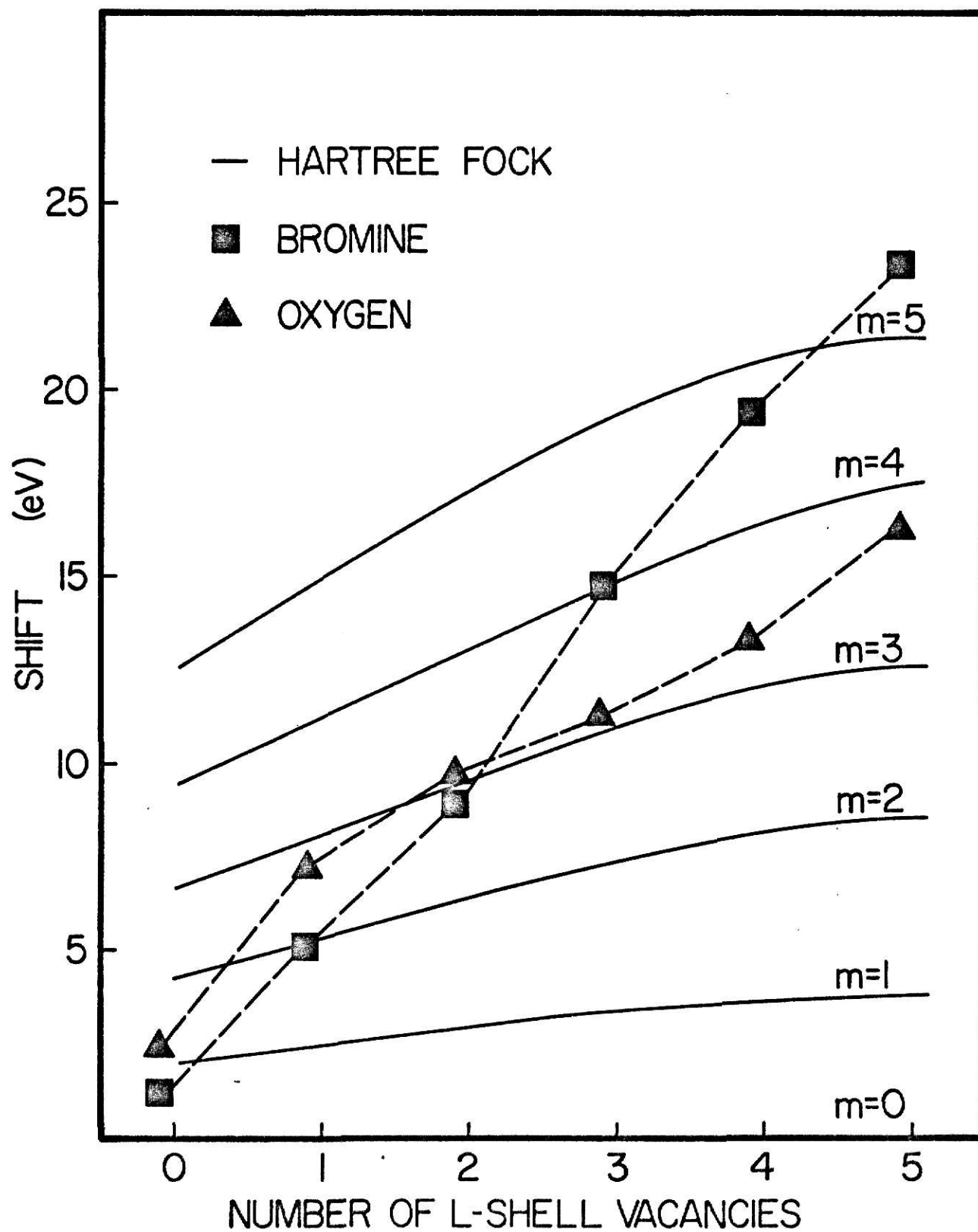
x-ray emission. The curved lines represent the HF calculations for M-shell defect configurations. Each curved line represents a different number of M-shell vacancies with 5 vacancies as the highest energy line and no vacancies being the horizontal axis. The squares are the actual measured Br induced energies minus the full M-shell  $K\alpha L^n$  HF calculated energy. The triangles are the published 0 induced energies of Hodge et al. minus the HF calculation. There are two interesting facts to be seen here. First, M-shell vacancies seem to increase with L-shell vacancies following bromine-ion impact. This fact is puzzling in itself but when one considers the second fact, that oxygen induced satellite peaks show a different trend in M-shell vacancies, one can conclude that this might be a collisional effect.

### C. Titanium

The original motivation for this experiment was to show that satellite structure could be resolved for bromine induced  $K\alpha$  x rays. By comparing the data of Kast et al. shown in Fig. 1 to the present study in Fig. 7, one can see that this goal has been realized. The first four satellite peaks are distinct with enough data points accumulated under the  $K\alpha L^4$  and  $K\alpha L^5$  peaks to fit the data to overlapping Gaussian peaks. The average number of L-shell vacancies is 2.2 as compared with 2.4 and 2.7 for Sc and Al respectively. The Ti value compares to a value of 2.4 deduced from the thin target titanium data of Kast et al. comparing  $K\alpha$  centroid shift and  $K\alpha/K\beta$  ratio. The effect in which the average number of L-shell vacancies decreases with increasing target atomic number is similar to observations<sup>9)</sup> with other heavy-ion beams. As with Sc, the

Figure 9: The shift of the titanium  $K\alpha L^n$  peak energies for Br and O bombardment compared to H-F calculations for  $m$  vacancies in the titanium M-shell.

# M-SHELL SHIFT FOR TITANIUM



relative intensities of the  $K\alpha L^n$  peaks more closely resemble the binomial type distribution of a  $P_L$  probability. The widths of these lines are approximately 50 eV wide or slightly more than double the resolution of the spectrometer.

The effects of M-shell vacancies for Ti (as shown in Table IV) closely parallel those for Sc. In both cases the HF configurations used to determine the different values in columns 3 and 5 were  $(1s)^2 (2s)^2 (2p)^{5-n} (3p)^{6-m} (4s)^2$  to  $(1s)^1 (2s)^2 (2p)^{6-n} (3p)^{6-m} (4s)^2$ . In this notation  $n$  refers to the number of L-shell vacancies before x-ray emission and  $m$  denotes the number of M-shell vacancies. As with Sc, the number of M-shell vacancies required to explain the experimentally determined energies increase with increasing L-shell vacancies. The energy shifts of Johnson et al.<sup>19)</sup> for  $O + Ti$  are listed showing a different trend in M-shell vacancies, again, suggesting that this is a collisional effect. Figure 9 shows the effect in the form of a graph similar to Figure 8. The squares represent the Br data and the triangles shift of the satellite peak energies measured by Johnson et al. In a recent article in Physical Review A, Watson et al.<sup>10)</sup> noted a similar effect using Cl beams.

Some insight to the cause of this effect may be gained by examining the recoil of the target atom. By calculating the transverse impulse given to the target nucleus, one can estimate the recoil energy for a given collision. After a collision with a 31 MeV Br ion which penetrated to the Ti K-shell, the Ti should recoil with about 40 keV of energy. A 30 MeV O ion would transfer only 0.5 keV of energy to the Ti atom. The recoil energies are quite different, but it is not very

probable that 40 keV Ti atoms change appreciably the  $K\alpha$  satellite spectrum. The fact that all the data of Sc and Ti bombarded by O and Br show increasing M-shell vacancies with increasing L-shell vacancies may be evidence for a shake-off effect. The more L-shell vacancies that are created, the greater the Coulomb impulse delivered to the M-shell electrons thereby increasing the probability for shake off of an M-shell electron. Molecular promotion may also offer a possible interpretation of the difference between the O and Br induced spectra. Ti is the light partner in the Br + Ti collision, but it is the heavy partner in an O + Ti collision. As the light partner in the Br collision, the L-shell of Ti is coupled to the 3p level in the united atom. The united atom is then coupled to the 3p in the Br ion. If a vacancy is present in the Br 3p level, electrons from the Ti L-shell can be promoted by this mechanism. In the solid target the actual charge state of Br ions is not known, but the average charge state for a 31 MeV Br ion is between +14 and +15. This would mean that a fraction of the Br ions has vacancies in the 3p level. If promotion is a dominate feature in the ionization of Ti, then by sampling Ti atoms with different amounts of L-shell vacancies, one might be considering different charge state distributions of impacting Br ions. Higher charge state Br ions are more likely to Coulomb ionize the Ti M-shell as well as promote the Ti L-shell electrons. Support for this model is gained by examining the scaled velocities (ion velocity/orbital electron velocity). The average L-shell orbital velocity of Ti is almost twice the velocity of a 31 MeV Br ion. In this scaled velocity region reasonable success has been attained with the molecular promotion

model. The M-shell electrons of Ti have a velocity of only half the ion's velocity and in this region Coulomb ionization is expected to be dominate. More experimental study on moderately slow, heavy-ion beams should provide more insight into the mechanisms responsible for the observed effects.

#### IV. CONCLUSION

To summarize, Br induced spectra from thick targets of Ti, Sc, and Al show structure that can be resolved into  $K\alpha L^n$  peaks by improving the resolution of Kast et al. The  $K\alpha L^n$  peaks of Al are clearly resolved for  $n=0$  to 5, however, the  $K\alpha L^n$  peaks of Sc and Ti are resolved only for states with  $n \leq 4$ . The average number of L-shell vacancies is seen to decrease with increasing target atomic number. All peaks are broadened and shifted to higher than normal energy due to the degree of M-shell ionization. The average number of M-shell vacancies required to explain the observed energies of the  $K\alpha$  satellite peaks increases with increasing L-shell ionization for Ti and Sc which is due to a collisional process. M-shell ionization is nearly the same for these two targets. Al shows very nearly equal intensities for 2, 3, and 4 L-shell vacancies and exhibits an approximately constant number of M-shell vacancies with varying L-shell ionization.

Insight into the process causing these effects could be gained by studying  $K\alpha$  x rays from targets between 20 and 30 with incident beams of F, Cl, Br, and I. Each of the beams represents a different full shell of electrons and is easily produced as a negative ion for Van de Graaff acceleration. Also, the experiment should be done for at least two matched velocities. This would give an indication of whether or not this effect is due to the effective charge of the beam ion or its speed. Another possibility is that this is a recoil effect. Performing this experiment with the similar target as a gas and as a solid should give an indication as to the importance of recoil effects.

Initial attempts at observing Ar  $K\alpha$  x rays with the Johansson spectrometer have been unsuccessful.

# REFERENCES

1. W. M. Coates, Phys. Rev. 46, 542 (1934).
2. P. Richard, I. L. Morgan, T. Furuta, and D. Burch, Phys. Rev. Lett. 23, 1009 (1969).
3. D. Burch and P. Richard, Phys. Rev. Lett. 25, 983 (1970).
4. A. R. Knudson, K. J. Nagel, P. G. Burkhalter, and K. L. Dunning, Phys. Rev. Lett. 26, 1149 (1971).
5. D. Burch, P. Richard, and R. L. Blake, Phys. Rev. Lett. 26, 1355 (1971).
6. Q. C. Kessel and B. Fastrup, Case Studies in Atomic Physics 3, 137 (1973).
7. J. D. Garcia, R. J. Fortner, and T. M. Kavanagh, Rev. Mod. Phys. 45, 111 (1973).
8. R. L. Kauffman, C. W. Woods, K. A. Jamison, and P. Richard, Phys. Letters 50A, 117 (1974).
9. R. L. Kauffman, J. H. McGuire, and P. Richard, Phys. Rev. A 8, 1233 (1973).
10. R. L. Watson, F. E. Jenson, and T. Chiao, Phys. Rev. A 10, 1230 (1974).
11. T. K. Li, R. L. Watson, and J. S. Hansen, Phys. Rev. A 8, 1258 (1973).
12. D. G. McCrary and P. Richard, Phys. Rev. A 5, 1249 (1972).
13. G. Bissinger, P. H. Nettles, S. M. Shafroth, and A. W. Waltner, Phys. Rev. A 10, 1932 (1974).
14. S. Datz, C. D. Moak, B. R. Appelton, and T. A. Carlson, Phys. Rev. Lett. 27, 363 (1971).

15. J. W. Kast, B. Budick, A. M. Rushton, L. Skoski, and H. J. Verschell, Phys. Rev. Lett. 32, 697 (1974).
16. C. Froese-Fischer, Comp. Phys. Comm. 1, 151 (1970).
17. F. Herman and S. Skillman, Atomic Structure Calculations (Prentice-Hall 1973).
18. B. Hodge, R. L. Kauffman, C. F. Moore, and P. Richard, J. Phys. B 6, 2468 (1973).
19. B. Johnson, M. Senglaub, P. Richard, and C. F. Moore, J. Physik 261, 413 (1974).
20. M. A. Blokhin, Methods of X-Ray Spectroscopic Research, edited by M. A. S. Ross (Pergamon Press 1965) p. 176.
21. J. A. Bearden, Rev. Mod. Phys. 31, 78 (1967).
22. W. Bambynek, B. Crasemann, R. W. Fink, H. U. Freund, H. Mark, C. D. Swift, R. E. Price, P. V. Rao, Rev. Mod. Phys. 44, 716 (1972).

TABLE I  
EXPERIMENTAL ENERGIES AND WAVELENGTHS FOR K $\alpha$  SATELLITES  
PRODUCED BY Br BOMBARDMENT

Target	Label	Energy <sup>a)</sup> (eV)	Wavelength (Å)	Relative Intensity	Average No. of L-Shell Vacancies
Ti	K $\alpha$ L <sup>0</sup>	4509.6	2.749	12.3	2.2
	K $\alpha$ L <sup>1</sup>	4535.7	2.733	17.1	
	K $\alpha$ L <sup>2</sup>	4563.3	2.717	28.7	
	K $\alpha$ L <sup>3</sup>	4593.6	2.699	25.1	
	K $\alpha$ L <sup>4</sup>	4623.8	2.681	12.5	
	K $\alpha$ L <sup>5</sup>	4655.1	2.663	4.3	
Sc	K $\alpha$ L <sup>0</sup>	4090.1	3.031	10.1	2.4
	K $\alpha$ L <sup>1</sup>	4113.9	3.014	15.3	
	K $\alpha$ L <sup>2</sup>	4140.9	2.994	29.6	
	K $\alpha$ L <sup>3</sup>	4170.7	2.973	24.6	
	K $\alpha$ L <sup>4</sup>	4200.1	2.952	15.3	
	K $\alpha$ L <sup>5</sup>	4228.3	2.932	5.0	
Al	K $\alpha$ L <sup>0</sup>	1488.2	8.331	11.9	2.7
	K $\alpha$ L <sup>1</sup>	1497.8	8.277	13.9	
	K $\alpha$ L <sup>2</sup>	1509.3	8.214	18.4	
	K $\alpha$ L <sup>3</sup>	1523.2	8.139	19.4	
	K $\alpha$ L <sup>4</sup>	1537.1	8.066	19.8	
	K $\alpha$ L <sup>5</sup>	1552.2	7.987	16.6	

<sup>a)</sup> Typical error is of the order of 0.5 eV for all of the states of Al whereas for Sc and Ti, the error is 1 eV for KL<sup>n</sup> states with  $n \leq 3$  and 3 eV for the KL<sup>n</sup> states with  $n \geq 4$ .

TABLE II

EFFECTS OF M-SHELL VACANCIES ON Al  $K\alpha$  SATELLITE PEAK ENERGIES

Peak Label	Shift <sup>a)</sup> (eV)	M-Shell Vacancies <sup>b)</sup>
$K\alpha L^0$	1.7	2
$K\alpha L^1$	1.5	2
$K\alpha L^2$	1.6	2
$K\alpha L^3$	2.6	1
$K\alpha L^4$	2.3	1
$K\alpha L^5$	1.5	1

a) Shift is defined as the difference between the experimental peak energy and the H-F calculation with all m-shell electrons present.

b) Error is expected to be  $\pm 0.5$ .

TABLE III

EFFECTS OF M-SHELL VACANCIES ON Sc K $\alpha$  SATELLITE PEAK ENERGIES

Peak Label	Bromine Induced		Oxygen Induced <sup>b)</sup>	
	Shift <sup>a)</sup> (eV)	M-Shell Vacancies <sup>c)</sup>	Shift <sup>a)</sup> (eV)	M-Shell Vacancies <sup>c)</sup>
K $\alpha$ L <sup>0</sup>	1.0	1	.9	1
K $\alpha$ L <sup>1</sup>	4.4	2	5.5	3
K $\alpha$ L <sup>2</sup>	9.7	3	9.6	3
K $\alpha$ L <sup>3</sup>	16.5	4	9.8	3
K $\alpha$ L <sup>4</sup>	21.5	5	11.4	3
K $\alpha$ L <sup>5</sup>	24.1	6	13.8	4

a) Shift is defined as the difference between the experimental peak energy and the H-F calculation with all m-shell electrons present.

b) Shift calculated from published energies given by ref. 18.

c) Error is expected to be  $\pm 0.5$ .

TABLE IV

EFFECTS OF M-SHELL VACANCIES ON Ti K $\alpha$  SATELLITE PEAK ENERGIES

Peak Label	Bromine Induced		Oxygen Induced <sup>b)</sup>	
	Shift <sup>a)</sup> (eV)	M-Shell Vacancies <sup>c)</sup>	Shift <sup>a)</sup> (eV)	M-Shell Vacancies <sup>c)</sup>
K $\alpha$ L <sup>0</sup>	.18	1	2.5	1
K $\alpha$ L <sup>1</sup>	5.0	2	7.2	3
K $\alpha$ L <sup>2</sup>	9.3	3	9.4	3
K $\alpha$ L <sup>3</sup>	14.9	4	11.2	3
K $\alpha$ L <sup>4</sup>	19.2	5	13.3	3
K $\alpha$ L <sup>5</sup>	23.2	6	15.4	4

a) Shift is defined as the difference between the experimental peak energy and H-F calculations with all m-shell electrons present.

b) Shift calculated from published energies given by ref. 19.

c) Error is expected to be  $\pm 0.5$ .

## APPENDIX

This appendix consists of the published form of this thesis. It appeared in Volume II, Number 2 of Physical Review A in February, 1975.

# $K\alpha$ satellite x rays in Al, Sc, and Ti following bromine-ion bombardment

K. A. Jamison, C. W. Woods, Robert L. Kauffman, and Patrick Richard

Kansas State University, Manhattan, Kansas 66506

(Received 3 July 1974)

A curved crystal spectrometer has been used to resolve structure in  $K\alpha$  x rays from thick targets of Al, Sc, and Ti following bromine-ion bombardment. We find that this structure is due to states with different numbers of  $L$ -shell vacancies. From this we can deduce the relative intensities for single  $K\alpha$  and multiple  $L$ -shell vacancy production as well as the number of  $M$ -shell vacancies of each  $KL^n$  configuration undergoing  $K\alpha$  x-ray emission. These results are compared to previous measurements with Br beams in which  $KL^n$  configurations could not be resolved.

## I. INTRODUCTION

High-resolution  $K$  x-ray spectra have been obtained previously for incident beams of H, He, Li, C, N, O, F, Ne, and Cl on several targets from Ne through Fe.<sup>1-11</sup> In these spectra single  $K\alpha$ , multiple  $L$ -shell ionization peaks have been resolved in both the  $K\alpha$  and  $K\beta$  transitions. Recently, Kast *et al.*<sup>12</sup> extended the study of  $K\alpha$  x-ray satellite production to bromine beams. They did not resolve distinct satellite structure in the  $K$  x rays from Ti and Mn when excited by bromine beams having energies from 12 to 97 MeV. They suggested that a greater variation of  $M$ -shell ionization by the large- $Z$  bromine projectile broadens the satellite lines to the point where they cannot be resolved with their reported resolution. We have found that with higher energy resolution the Ti satellite structure can be observed but the individual satellites are broadened. In this paper we report measurements which resolve  $K\alpha$  satellite lines in Al, Sc, and Ti from 31-MeV Br and 2-MeV  $H^+$  bombardment. The observed energies and relative intensities of the satellite lines have been extracted from the data. The effect of  $M$ -shell vacancies on the  $K\alpha$  transition energies is investigated by comparing Hartree-Fock calculations<sup>13</sup> to the measured Br-induced  $K\alpha$  energies as well as to the 2-MeV  $H^+$ -induced  $K\alpha$  energies. From these comparisons it is found that the number of  $M$ -shell vacancies is dependent on the number of  $L$ -shell vacancies at the time of  $K\alpha$  x-ray emission and that the average number of  $L$ -shell vacancies decreases with increasing target  $z$ .

## II. EXPERIMENTAL SETUP

A 4-in. curved crystal spectrometer<sup>14</sup> with a flow proportional detector was used to observe x rays from thick targets of Al, Sc, and Ti produced by collisions with incident Br ions. A 31-MeV Br<sup>17</sup> beam was obtained from the Kansas State tandem Van de Graaff accelerator. Typical beam currents throughout were on the order of 1  $\mu$ A. The  $K$  x

rays of Ti and Sc were analyzed in first order with a LiF crystal with a  $2d$ -spacing of 4.027 Å. Al x rays were analyzed in first order with an ADP (ammonium dihydrogen phosphate) crystal,  $2d$  spacing of 10.640 Å. In each case the x-ray proportional detector used a  $P$ -10 gas mixture (10% methane, 90% argon) with a thin ( $\sim 5000$ -Å) polypropylene window. The spectrometer stepping motor was controlled by an on-line PDP-15 computer and at each angular setting of the crystal and detector the number of x rays was recorded for a given number of  $\mu$ C of beam on the thick metallic targets. The step size for the Ti and Sc spectra was 0.000 212 Å and for the Al spectrum it was 0.000 560 Å. In each case approximately 1000 data points were taken and then compressed by 5 into 200 channels for later off-line analysis. Each spectrum was repeated at least once and all reproduced to within statistical errors. The statistical uncertainty in each data point was approximately 3% for the  $K\alpha L^n$  peaks<sup>15</sup> produced by Br bombardment and approximately 1% for the  $K\alpha L^0$  peak produced by  $H^+$  bombardment.

The spectra were calibrated using the normal  $K\alpha$  and  $K\beta$  transitions<sup>16</sup> seen under 2.0-MeV  $H^+$  bombardment. Resolution [full width half-maximum (FWHM) of the  $H^+$ -induced  $K\alpha$  line] was 2.5, 11.0, and 24.0 eV for the Al, Sc, and Ti, respectively. Kast *et al.*<sup>12</sup> reported a resolution of 44 eV for Ti in second order and 32 eV for Mn in third order using a graphite mosaic crystal spectrometer.

## III. RESULTS

Figures 1, 2, and 3 show the spectra of Al, Sc, and Ti, respectively, for Br and  $H^+$  excitation. In each case the proton calibration spectrum is overlaid with the bromine-induced spectrum. A  $\chi^2$  fit with Gaussian peaks was used to extract peak positions and relative intensities from the spectra. These best-fit values together with the proton calibration spectra were used to obtain the energies, wavelengths, relative intensities, and average  $L$ -shell vacancies listed in Table I. In the Sc and Ti

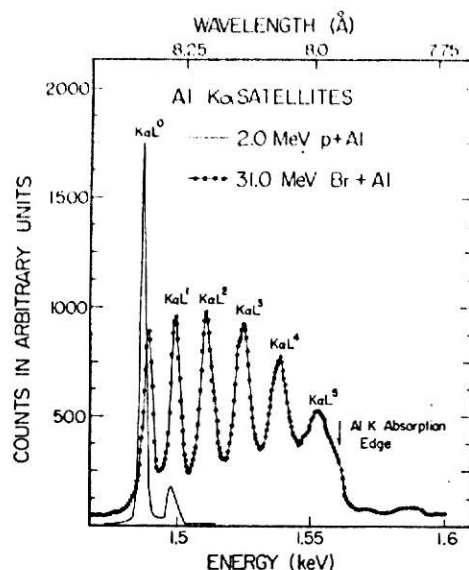


FIG. 1. Aluminum  $K\alpha$  x-ray spectra resulting from collisions with 31.0-MeV bromine ions and 2.0-MeV  $H^+$ . The  $H^+$ -induced spectrum contains approximately 20 times as many counts as the Br-induced spectrum. The Al  $K$  absorption edge is due to self-absorption in the thick target.

cases we find that the average number of  $L$ -shell vacancies before a  $K\alpha$  transition are 2.4 and 2.2, respectively, following bromine excitation, which

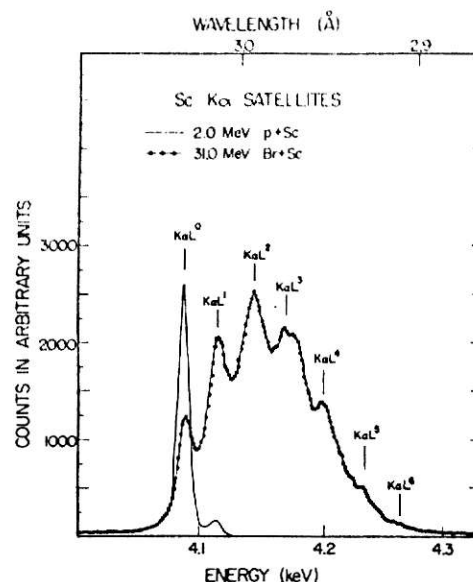


FIG. 2. Scandium  $K\alpha$  x-ray spectra after collisions with 31.0-MeV bromine ions and 2.0-MeV  $H^+$ . The proton-induced spectrum contains approximately 15 times as many counts as the Br-induced spectrum.

agrees with an interpolated value of 2.4  $L$ -shell vacancies deduced by Kast *et al.*<sup>12</sup> for Ti. The widths (FWHM) of the Br-induced  $K\alpha$  satellite lines are very nearly double the resolution of the spectrometer for Sc and Ti. In the Al data we find that

TABLE I. Energies and wavelengths for  $K\alpha$  satellites produced by Br bombardment.

Target	Label	Energy <sup>a</sup> (eV)	Wavelength (Å)	Relative intensity (%)	Average number of $L$ -shell vacancies	
					Present	Kast <i>et al.</i> <sup>b</sup>
Ti	$K\alpha L^0$	4509.6	2.749	12.3		
	$K\alpha L^1$	4535.7	2.733	17.1		
	$K\alpha L^2$	4563.3	2.717	28.7		
	$K\alpha L^3$	4593.6	2.699	25.1	2.2	2.4
	$K\alpha L^4$	4623.8	2.681	12.5		
	$K\alpha L^5$	4655.1	2.663	4.3		
Sc	$K\alpha L^0$	4090.1	3.031	10.1		
	$K\alpha L^1$	4113.9	3.014	15.3		
	$K\alpha L^2$	4140.9	2.994	29.6		
	$K\alpha L^3$	4170.7	2.973	24.6	2.4	...
	$K\alpha L^4$	4200.1	2.952	15.1		
	$K\alpha L^5$	4228.3	2.932	3.5		
	$K\alpha L^6$	4249.2	2.918	1.8		
Al	$K\alpha L^0$	1488.2	8.331	11.9		
	$K\alpha L^1$	1497.8	8.277	13.9		
	$K\alpha L^2$	1509.3	8.214	18.4		
	$K\alpha L^3$	1523.2	8.139	19.4	2.7	...
	$K\alpha L^4$	1537.1	8.066	19.8		
	$K\alpha L^5$	1552.2	7.987	16.6		

<sup>a</sup>Typical error is of the order of 0.5 eV for all of the states of Al whereas for Sc and Ti, the error is  $\sim 1$  eV for  $KL^n$  states with  $n \leq 3$  and  $\sim 3$  eV for the  $KL^n$  states with  $n \geq 4$ .

<sup>b</sup>Value deduced from thin-target data by comparing  $K\alpha$  centroid shift and  $K\alpha/K\beta$  ratio.

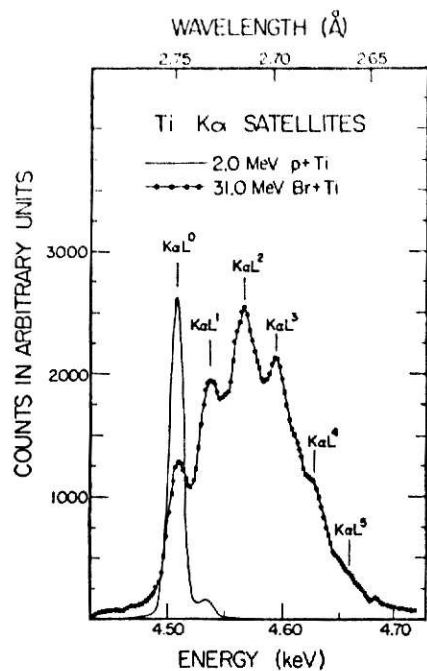


FIG. 3. Titanium  $K\alpha$  x-ray spectra after collisions with 31.0-MeV bromine and 2.0-MeV  $H^+$ . The proton-induced spectra contains approximately 15 times as many counts as the Br-induced spectrum.

the average number of  $L$ -shell vacancies is 2.7 even though the relative intensities for 2, 3, and 4  $L$ -shell vacancies are nearly equal. The resolution of the bromine-induced lines for Al is approximately 1.6 times that of the proton data. It should be noted in Fig. 1 that the Al  $K$  absorption edge causes a sharp decrease in intensity above the  $K\alpha L^5$  peak. This is due to self-absorption in the thick target. The normal  $K\beta$  peak of Al falls just below the absorption edge and very near the  $K\alpha L^5$  peak. Although the  $K\beta$  intensity is expected to be very small, its presence together with the proximity of the absorption edge makes it difficult to extract accurately the  $K\alpha L^5$  peak position and intensity. For these cases of Al, Sc, and Ti it is found that the higher the target  $z$  the lower the average number of  $L$ -shell vacancies at the time of x-ray emission. This agrees with the observation of Kast *et al.*<sup>12</sup>

Table II summarizes the effects of  $M$ -shell vacancies on the  $K\alpha$  satellite peak positions produced by Br. The average number of  $M$ -shell vacancies associated with each state of single  $K$ -shell plus  $n$   $L$ -shell vacancies is deduced. The normal  $K\alpha$  transition produced in  $H^+$  bombardment is used to normalize Hartree-Fock (HF) self-consistent-field calculations.<sup>17</sup> It was assumed that 2-MeV protons produced no  $M$ -shell vacancies in the  $K\alpha L^0$  peak. The normalized HF energies were used to extract the energy shifts of all of the  $K\alpha L^n$  peaks produced by bromine. These numbers are tabulated in col-

TABLE II. Average number of  $M$ -shell vacancies required to fit  $K\alpha L^n$  peak energies.

Target	Label	Shift <sup>a</sup> (eV)	$M$ -shell vacancies		
			Present <sup>b</sup>	Oxygen <sup>c</sup>	Kast <i>et al.</i> <sup>d</sup>
Ti	$K\alpha L^0$	.8	1	1	
	$K\alpha L^1$	5.0	2	3	
	$K\alpha L^2$	9.3	3	3	3.2
	$K\alpha L^3$	14.9	4	3	
	$K\alpha L^4$	19.2	5	3	
	$K\alpha L^5$	23.2	6	4	
Sc	$K\alpha L^0$	1.0	1	1	
	$K\alpha L^1$	4.4	2	3	
	$K\alpha L^2$	9.7	3	3	
	$K\alpha L^3$	16.5	4	3	
	$K\alpha L^4$	21.5	5	3	
	$K\alpha L^5$	24.1	6	4	
Al	$K\alpha L^0$	1.7	2		
	$K\alpha L^1$	1.5	2		
	$K\alpha L^2$	1.6	2		
	$K\alpha L^3$	2.6	1		
	$K\alpha L^4$	2.3	1		
	$K\alpha L^5$	1.5	1		

<sup>a</sup> The shift for a given  $K\alpha L^n$  state is the difference between the experimental energy from Br bombardment and the Hartree-Fock energy adjusted to agree with the experimental energy of  $K\alpha L^0$  from  $H^+$  bombardment.

<sup>b</sup> In this column the average number of  $M$ -shell vacancies required to explain the shifts in column 3 are tabulated. All vacancies are assumed to be in the  $3p$  subshell.

<sup>c</sup> Calculated values comparing oxygen induced x-ray energies, Refs. 8 and 18, to present HF calculations.

<sup>d</sup> Value deduced from thin-target data by comparing  $K\alpha$  centroid shift and  $K\alpha/K\beta$  ratio. Only vacancies from  $3p$  subshells are tabulated. Kast *et al.* require one additional  $3d$  and one additional  $4s$  vacancy.

umn 3 of Table II. Extensive HF calculations were performed in order to determine the energy shifts due to  $M$ -shell vacancies associated with each  $K\alpha L^n$  peak. The transitions calculated for Ti and Sc were  $(1s)^2(2s)^2(2p)^{5-n}(3s)^2(3p)^{6-m}(4s)^2 - (1s)(2s)^2(2p)^{6-n}(3s)^2(3p)^{6-m}(4s)^2$ . For Al the configurations  $(1s)^2(2s)^2(2p)^{5-n}(3s)^{2-m}$  and  $(1s)(2s)^2(2p)^{6-n}(3s)^{2-m}$  were calculated and energy differences determined. In this notation  $n$  refers to the number of  $L$ -shell vacancies before the transition has occurred and  $m$  refers to the number of  $M$ -shell vacancies. For the purpose of the calculations the conduction electrons were assumed to be absent although calculations showed it should make very little difference in the transition energy. Kast *et al.* assumed equally spaced peaks for each of the  $K\alpha L^n$  transitions and then used the  $K\alpha$  to  $K\beta$  ratio to calculate  $L$ - and  $M$ -shell vacancy production. Under higher resolution we see an increasing energy shift due to greater  $M$ -shell ioni-

zation for the higher  $K\alpha L^n$  peaks. This increasing energy shift (as shown in Table II) indicates that the assumption of equally spaced  $KL^n$  peaks used by Kast *et al.* is in error.

Column 4 of Table II shows the required number of  $M$ -shell vacancies to explain the shift in energy for each  $KL^n$  peak. It is noted that for Sc and Ti  $M$ -shell ionization increases directly with  $L$ -shell vacancies. A similar analysis of oxygen-induced x-ray energies for Ti, Johnson *et al.*<sup>18</sup> and for Sc, Hodge *et al.*<sup>9</sup> is listed in column 5 of Table II.  $M$ -shell ionization at the time of x-ray emission following oxygen bombardment is nearly constant for  $KL^1$  through  $KL^5$ . The difference in the trends of the number of  $M$ -shell vacancies between Br and O bombardment suggests that increasing  $M$ -shell ionization with  $L$ -shell vacancies is a collisional effect.

#### IV. CONCLUSION

In summary we have found that Br-induced spectra from thick targets of Ti, Sc, and Al show structure that can be resolved into  $K\alpha L^n$  peaks. The  $K\alpha L^n$  peaks of Al are clearly resolved for  $n = 0-5$ , however the  $K\alpha L^n$  peaks of Sc and Ti are resolved only for states with  $n > 4$ . All peaks are broadened and shifted to higher than normal energy due to the degree of  $M$ -shell ionization. We can conclude that the  $M$ -shell ionization increases with  $L$ -shell ionization for Ti and Sc which is due to a collisional process and that  $M$ -shell ionization is nearly the same for these two targets. Al shows nearly equal relative intensities for 2, 3, and 4  $L$ -shell vacancies and exhibits a slight decrease in  $M$ -shell vacancies with increasing  $L$ -shell ionization.

\*Work supported in part by the U. S. Atomic Energy Commission under Contract No. AT(11-1)-2130.

<sup>1</sup>Forrest Hopkins, D. O. Elliott, C. P. Bhalla, and Patrick Richard, Phys. Rev. A **8**, 2952 (1973).

<sup>2</sup>Robert L. Kauffman, James H. McGuire, Patrick Richard, and C. Fred Moore, Phys. Rev. A **8**, 1233 (1973).

<sup>3</sup>D. G. McCrary and Patrick Richard, Phys. Rev. A **5**, 1249 (1972).

<sup>4</sup>M. D. Brown, J. R. Macdonald, Patrick Richard, J. R. Mowat, and I. A. Sellin, Phys. Rev. A **9**, 1470 (1974).

<sup>5</sup>A. R. Knudson, D. J. Nagel, P. G. Burkhalter, K. L. Dunning, Phys. Rev. Lett. **26**, 1149 (1971).

<sup>6</sup>T. K. Li, R. L. Watson, and J. S. Hansen, Phys. Rev. A **8**, 1258 (1973).

<sup>7</sup>D. G. McCrary, M. Senglaub, and Patrick Richard, Phys. Rev. A **6**, 263 (1972).

<sup>8</sup>Bill Hodge, Robert Kauffman, C. Fred Moore, and Patrick Richard, J. Phys. B **6**, 2468 (1973).

<sup>9</sup>D. Burch and Patrick Richard, Phys. Rev. Lett. **26**,

1335 (1971).

<sup>10</sup>Robert L. Kauffman, Forrest Hopkins, C. W. Woods, and Patrick Richard, Phys. Rev. Lett. **31**, 621 (1973).

<sup>11</sup>C. F. Moore, M. Senglaub, B. Johnson, and P. Richard, Phys. Lett. **40A**, 107 (1972).

<sup>12</sup>J. W. Kast, B. Budick, A. M. Rushton, L. Skoski, and H. J. Verschell, Phys. Rev. Lett. **32**, 697 (1974).

<sup>13</sup>C. F. Fischer, Comput. Phys. Commun. **1**, 151 (1970).

<sup>14</sup>J. L. Jones, K. W. Paschen, and J. B. Nicholson, Appl. Opt. **2**, 955 (1963).

<sup>15</sup>The notation  $K\alpha L^n$  refers to a  $K\alpha$  transition from an initial state with  $n$   $L$ -shell vacancies.

<sup>16</sup>J. A. Bearden, Rev. Mod. Phys. **31**, 78 (1967).

<sup>17</sup>The calculated values of the  $K\alpha L^n$  transition energies for all three cases (Al, Sc, and Ti) were  $\sim 0.5\%$  below the  $H^+$  induced experimental values.

<sup>18</sup>B. M. Johnson, M. Senglaub, P. Richard, and C. F. Moore (unpublished).

STUDY OF K $\alpha$  X RAYS FROM Al, Sc, AND Ti  
FOLLOWING BROMINE-ION BOMBARDMENT

by

KEITH A. JAMISON

B.S., Kansas State University, 1973

---

AN ABSTRACT OF A MASTER'S THESIS

submitted in partial fulfillment of the

requirements for the degree

MASTER OF SCIENCE

Department of Physics

KANSAS STATE UNIVERSITY  
Manhattan, Kansas

1975

## ABSTRACT

A four-inch Johansson curved crystal spectrometer has been used to resolve structure in  $K\alpha$  x rays from thick targets of Al, Sc, and Ti following bromine-ion bombardment. The  $K\alpha L^n$  x-ray structure is due to states with different numbers of L-shell vacancies. These results are compared to previous measurements with Br beams in which  $K\alpha L^n$  configurations could not be resolved. From the resolved  $K\alpha L^n$  peaks the relative intensities can be deduced for single K-, multiple L-shell vacancy production. By comparing  $K\alpha L^n$  peak energies to Hartree-Fock calculations, the number of M-shell vacancies for each  $K\alpha L^n$  configuration undergoing  $K\alpha$  x-ray emission can be determined.